Time-dependent density functional theory of narrow band gap semiconductors using a screened range-separated hybrid functional

Dahvyd Wing,¹ Jeffrey B. Neaton,^{2,3,4,5} and Leeor Kronik¹

Department of Materials and Interfaces, Weizmann Institute of Science, Rehovoth 76100, Israel
Department of Physics, University of California, Berkeley, Berkeley, California 94720, USA
Materials Sciences Division, Lawrence Berkeley National Laboratory, Berkeley, California 94720, USA
Molecular Foundry, Lawrence Berkeley National Laboratory, Berkeley, CA 94720, USA
Kavli Energy NanoSciences Institute at Berkeley, Berkeley, CA, 94720, USA

Predicting the band structure and optical absorption spectra of narrow band gap semiconductors is challenging for electronic structure methods. Here, we show that density functional theory (DFT) can yield accurate band structures and time-dependent density functional theory (TDDFT) can yield accurate optical absorption spectra for these systems. This is achieved by using a screened range-separated hybrid (SRSH) functional with a single empirical parameter, fit to reproduce the experimental band gap. By comparing TDDFT results based on the SRSH approach with those obtained with the Heyd-Scuseria-Ernzerhof (HSE) functional we show that screened long-range exact exchange improves the accuracy of the TDDFT spectra for these systems.

The optical absorption spectra of narrow band gap semiconductors (i.e., those with a band gap smaller than ~ 0.8 eV) are often challenging to predict. A standard technique to calculate optical absorption spectra is to use many-body perturbation theory with the GW approximation [1–6] and the Bethe-Salpeter equation (BSE) [7–10] approach. While the GW-BSE approach is known for its accuracy, it can exhibit sensitivity to the density functional theory (DFT) starting point. For narrow band gap semiconductors, a challenge is that semilocal functionals, often used to generate a starting point for GW calculations, spuriously predict a metallic ground state [11–14] and even use of a self-consistent scheme does not result in sufficiently accurate band gaps [15–18].

Two approaches for overcoming this difficulty have been suggested. In one, the Tran-Blaha modified Becke-Johnson potential was found to yield reasonable band gaps for these materials [19–21]. However, using this approach as a starting point for "one-shot" GW calculations tends to yield overestimated band gaps [22]. In a different approach, hybrid functionals have been used to generate starting points for GW calculations. However, hybrid functionals predict a range of band gaps, depending on the amount of exact exchange included, thereby affecting subsequent "one-shot" GW results [12, 23, 24]. Specifically, the Heyd-Scuseria-Ernzerhof (HSE) [25] shortrange hybrid functional yields accurate results for narrow band gap semiconductors, but GW using it as a starting point produces results of similar quality only if selfconsistency is employed [26, 27]. A method to a priori select the right parameters of hybrid functionals for band gap prediction and for generating GW starting points remains an active area of research [28–33]. These issues have hampered the application of GW-BSE to narrow band gap (and other) semiconductors.

Time-dependent density functional theory (TDDFT) [34–37] in principle can yield accurate optical absorption spectra. However for crystalline solids TDDFT using (semi)local functionals produces inaccurate spectra

which are red-shifted and underestimate excitonic contributions to absorption peaks [38, 39], as can be seen in the optical absorption spectra of narrow band gap semiconductors in Ref. [40]. Many methods have been proposed to overcome these deficiencies [35], and several methods have been used to calculate the optical absorption of germanium [41–44] or indium arsenide [45], but to our knowledge only the jellium-with-gap (JGM) kernel with an empirical scissor shift has been tested on a set of narrow band-gap semiconductors [46]. In that work, reasonable results were obtained, however spin-orbit coupling effects were neglected.

TDDFT using hybrid functionals or other forms of screened exact exchange has received much attention recently as a promising way to calculate the optical absorption spectra of crystalline solids [47–55], but to our knowledge they have yet to be applied to narrow band gap semiconductors. In previous work [48, 50] we showed that DFT and TDDFT using the screened rangeseparated hybrid (SRSH) functional can produce band structures and optical absorption spectra on par with GW and GW-BSE, respectively, for a range of group IV and III-V semiconductors. In that work, a single parameter in the SRSH functional was fit to reproduce the quasiparticle band gap predicted by GW. Subsequent TDDFT calculations used a kernel obtained from the second functional derivative of the SRSH functional and no further fitting was required when calculating the TDDFT spectra. Given the success of our previous work and the advantages of the SRSH formalism, here we investigate whether the SRSH functional can accurately calculate band structures and optical absorption spectra for the narrow band gap semiconductors Ge, GaSb, InAs, and InSb.

In the SRSH functional, [28, 48] the exchange part of the Coulomb interaction is partitioned using the identity

$$\frac{1}{r} = \frac{\alpha + \beta \operatorname{erf}(\gamma r)}{r} + \frac{1 - [\alpha + \beta \operatorname{erf}(\gamma r)]}{r}, \quad (1)$$

where the first term is treated explicitly by a Fock-

like operator and the second term is approximated by semi-local exchange, in our case based on the Perdew-Burke-Ernzerhof (PBE) exchange-correlation functional [56]. The full form of the SRSH exchange-correlation functional can then be expressed as:

$$\begin{split} E_{xc}^{\text{SRSH}} &= (1 - \alpha) E_{KSx}^{SR} + \alpha E_{xx}^{SR} + [1 - (\alpha + \beta)] E_{KSx}^{LR} \\ &\quad + (\alpha + \beta) E_{xx}^{LR} + E_{KSc}, \quad (2) \end{split}$$

where the subscripts KSx and KSc denote (semi)local KS exchange and correlation, respectively, and xx is exact (Fock) exchange. In this form, the Fock-like exchange operator is naturally partitioned into short-range (SR) and long-range (LR) components that are scaled by the error function such that there is seamless transition between the two regimes. α , β , and γ are parameters. α controls the fraction of short-range exact exchange, $\alpha+\beta$ controls the fraction of long-range exact exchange, and γ is the range-separation parameter that controls the transition from the short-range to long-range regimes.

In this study we use the Vienna *ab initio* simulation package (VASP), a plane-wave code,[57] with PBE-based projector-augmented waves (PAWs) for treating core electrons [58]. For gallium, germanium, and indium the PAWs include semi-core *d*-states. We use the room-temperature lattice parameter for all materials. All calculations, including the fitting procedure, include spin-orbit coupling effects self-consistently.

We select parameters for the SRSH functional in the following way. We set $\alpha = 0.25$ in Eq. (1), as is done in the HSE functional (note that this choice is not unique, see the supplementary material of ref. 50). We then set the β and γ parameters using a two-step procedure.

First, we calculate the high-frequency dielectric constant, ϵ_{∞} , and set β so that $\alpha + \beta = \frac{1}{\epsilon_{\infty}}$. This constraint on β ensures that the SRSH functional has the correct $\frac{1}{\epsilon_{\infty}r}$ asymptotic behavior. The ion-clamped, highfrequency dielectric constant, ϵ_{∞} , is calculated from the change in polarization in response to a finite electric field [59, 60]. The HSE functional is used for this calculation, as it has been shown to lead to relatively accurate dielectric constants [47, 50]. Due to the fact that the semiconductors in this study have large dielectric constants. SRSH band structures and optical spectra of semiconductors are not strongly affected by the exact value of the dielectric constant, as long as the SRSH functional is fitted to the fundamental band gap of the material [50]. Thus the choice of which functional to use to calculate the dielectric constant is of little consequence. In these calculations local field effects are included for both Hartree and exchange-correlation potentials [61]. The plane wave cutoff is 300 eV for all materials and an $8\times8\times8$ ($9\times9\times9$ for germanium) Monkhorst-Pack Γ centered k-grid is used. The total energy convergence criteria for calculations where the small electric field is applied is 10^{-10} eV. With these parameters the dielectric constant is converged to within 3%. Our calculated dielectric constants are reported in Table I.

Second, we fit the range-separation parameter, γ to obtain the experimental room-temperature fundamental band gap [62]. A priori selection of all the parameters of the SRSH functional is an ongoing challenge [28–33]. Here, the same numerical parameters were used as in the dielectric response, except that the total energy convergence was reduced to 10^{-4} eV. This converged the band gap to within 0.03 eV for all materials. The resulting range-separation parameters are reported in Table I.

TABLE I. Room temperature experimental lattice constants [62], ion-clamped dielectric constants using the HSE functional, experimental high-frequency dielectric constants for comparison [62], SRSH range-separation parameters that yield the experimental room-temperature fundamental band gap [62], and fundamental band gaps calculated by HSE. In all calculations spin-orbit coupling effects were included.

	a_{lat} (Å)	$\epsilon_{\infty}^{\mathrm{theory}}$	$\epsilon_{\infty}^{\mathrm{expt}}$	$\gamma (\mathring{\mathrm{A}}^{-1})$	$E_{\rm g,expt}$ (eV)	$E_{\rm g,HSE}$
Ge	5.66	14.8	16.0	0.41	0.67	0.71
GaSb	6.10	13.1	14.5	0.31	0.75	0.70
InAs	6.06	11.4	12.4	0.45	0.36	0.38
InSb	6.48	13.2	15.7	0.50	0.18	0.28

TDDFT calculations are performed by solving the linear response equations [63–65] within the Tamm-Dancoff approximation [36, 66]. For a detailed discussion of the equations in the TD-SRSH case, see Refs. 48 and 67. These calculations use a planewave energy cutoff of 240 eV for Ge, 220 eV for GaSb, and 180 eV for InAs and InSb. Additionally, the exchange-correlation kernel is evaluated using six valence bands and six conduction bands, the transition energy cutoff is set to 10 eV, and a Gaussian broadening of 0.1 eV is used. These parameters converge the first two absorption peaks of the optical absorption peak heights to within 3%. Calculations use a $14 \times 14 \times 14$ k-grid with a judiciously chosen k-grid shift (0.1, 0.45, 0.75) selected to rapidly converge the TDDFT results by maximizing the sampling of different transition energies, as described in Ref. 50.

Band structures are calculated using the Wanniers90 software package [68] using the same plane wave energy cutoffs and dense k-grid as the TDDFT calculations. These parameters converge the band gap to 0.03 eV, though Wannierization introduces an error of up to 0.1 eV when interpolating to k-points not sampled.

In Figure 1, we present the SRSH band structures for these semiconductors and compare them to those obtained using the empirical pseudopotential method (EPM) [69, 70], often used as benchmark data. Importantly, agreement between the two methods is good for the top-most valence bands and bottom-most conduction bands, which are the most important bands for TDDFT calculations. The bottom SRSH valence bands are significantly stretched as compared to the EPM, similar to results comparing SRSH and GW band structures [50]. In the case of Ge, SRSH predicts a direct band gap of 0.69 eV, which is marginally larger than the fitted indirect band gap, and is somewhat smaller than the

perimental direct band gap of 0.8 eV [62]. The direct band gap of Ge is also reported to be underestimated in a prior set of GW calculations, possibly due to an insufficient number of semi-core electrons [14]. Additionally, the SRSH direct band gaps shown in Fig. 1, in particular that of InSb, are somewhat smaller than the values obtained from SRSH calculations using a Monkhorst-Pack Γ -centered k-grid, as reported in Table I. This is due to using Wannier interpolation for the Γ point which is not included in the shifted k-grid.

In Figure 2, we present the TDDFT optical absorption spectra of SRSH compared to room-temperature experimental measurements [71]. The agreement between theory and experiment is very good. In particular, SRSH correctly captures the spin-orbit splitting of the first absorption peak for GaSb and InSb (the smaller splitting of the first peak in InAs likely requires a larger k-grid to be resolved). GaSb peaks are shifted by 0.2 eV compared to experiment. An overestimate of the experimental band gap used to fit SRSH could cause such as shift, but the literature is in agreement on the value of the band gap [62, 72–75]. Averaging across the results of all four materials, SRSH blue shifts the first and second absorption peaks by 0.11 ± 0.08 eV.

For comparison, we also include the optical absorption spectra of HSE in Figure 2, which is somewhat blue-shifted from SRSH and experiment. The somewhat smaller blue-shift for GaSb and larger blue-shift for InSb can be explained by noting that HSE underestimates the ground state band gap for GaSb and overestimates the band gap for InSb, see Table I. The HSE spectra are on average 0.09 ± 0.03 eV blue shifted compared to SRSH spectra, as calculated by the difference between the position of the first peak of the HSE and SRSH spectra minus the difference between the HSE and SRSH band gaps. We hypothesize that the blue shift of the HSE spectra is due to the neglect of screened long-range exact

exchange, which leads to incorrect asymptotic behavior of the exchange-correlation kernel in the long-wavelength limit [38, 39, 48]. Without the correct asymptotic behavior excitonic effects are not properly accounted for. These excitonic effects red shift the absorption spectra and increase the first absorption peak, relative to the independent particle absorption spectra, for IV and III-V semiconductors [8, 39, 76]. Interestingly, the first absorption peak calculated by HSE is shifted, but of similar intensity to that of SRSH. We have also observed a similar effect in the case of silicon.

In conclusion, by empirically fitting one parameter of the SRSH functional to the experimental band gap, we show that the SRSH functional is able to yield accurate band structures and optical absorption spectra for four challenging narrow band gap semiconductors. We also show by comparing the TDDFT SRSH spectra to the HSE spectra that even for materials which have large high-frequency dielectric constants, including screened long-range exact exchange improves the optical absorption spectra. TDDFT using the SRSH functional is a useful pragmatic approach given that standard non-empirical methods typically fail to yield accurate results for these materials.

This work was primarily supported via a US-Israel National Science Foundation - Binational Science Foundation (NSF-BSF) grant, DMR-1708892. Partial support from the Theory Program at the Lawrence Berkeley National Laboratory through the Office of Basic Energy Sciences, U.S. Department of Energy, under Contract No. DE-AC02-05CH11231, was also provided. Computational resources were provided by the National Energy Research Scientific Computing Center and the Molecular Foundry, DOE Office of Science User Facilities supported by the Office of Science of the U.S. Department of Energy under Contract No. DE-AC02-05CH11231.

L. Hedin, Phys. Rev. 139, A796 (1965).

^[2] L. Hedin and S. Lundqvist (Academic Press, 1970) pp. 1 – 181

^[3] M. S. Hybertsen and S. G. Louie, Phys. Rev. Lett. 55, 1418 (1985).

^[4] M. S. Hybertsen and S. G. Louie, Phys. Rev. B 34, 5390 (1986).

^[5] F. Aryasetiawan and O. Gunnarsson, Rep. Prog. Phys. 61, 237 (1998).

^[6] D. Golze, M. Dvorak, and P. Rinke, Front. Chem. 7, 377 (2019).

^[7] G. Strinati, Riv. Nuovo Cimento 11, 1 (1988).

^[8] M. Rohlfing and S. G. Louie, Phys. Rev. Lett. 81, 2312

^[9] M. Rohlfing and S. G. Louie, Phys. Rev. B 62, 4927 (2000).

^[10] G. Onida, L. Reining, and A. Rubio, Rev. Mod. Phys. 74, 601 (2002).

^[11] M. van Schilfgaarde, T. Kotani, and S. V. Faleev, Phys.

Rev. B 74, 245125 (2006).

^[12] F. Fuchs, J. Furthmüller, F. Bechstedt, M. Shishkin, and G. Kresse, Phys. Rev. B 76, 115109 (2007).

^[13] T. Kotani and M. van Schilfgaarde, Solid State Commun. 121, 461 (2002), see band gap of InN.

^[14] B. D. Malone and M. L. Cohen, J. Phys.: Condens. Matter 25, 105503 (2013).

^[15] A. N. Chantis, M. van Schilfgaarde, and T. Kotani, Phys. Rev. Lett. 96, 086405 (2006).

^[16] D. Deguchi, K. Sato, H. Kino, and T. Kotani, Japanese Journal of Applied Physics 55, 051201 (2016).

^[17] M. Grumet, P. Liu, M. Kaltak, J. Klimes, and G. Kresse, Phys. Rev. B 98, 155143 (2018).

^[18] Z. Taghipour, E. Shojaee, and S. Krishna, Journal of Physics: Condensed Matter 30, 325701 (2018).

^[19] Y.-S. Kim, M. Marsman, G. Kresse, F. Tran, and P. Blaha, Phys. Rev. B 82, 205212 (2010).

^[20] H. Jiang, The Journal of Chemical Physics 138, 134115 (2013).

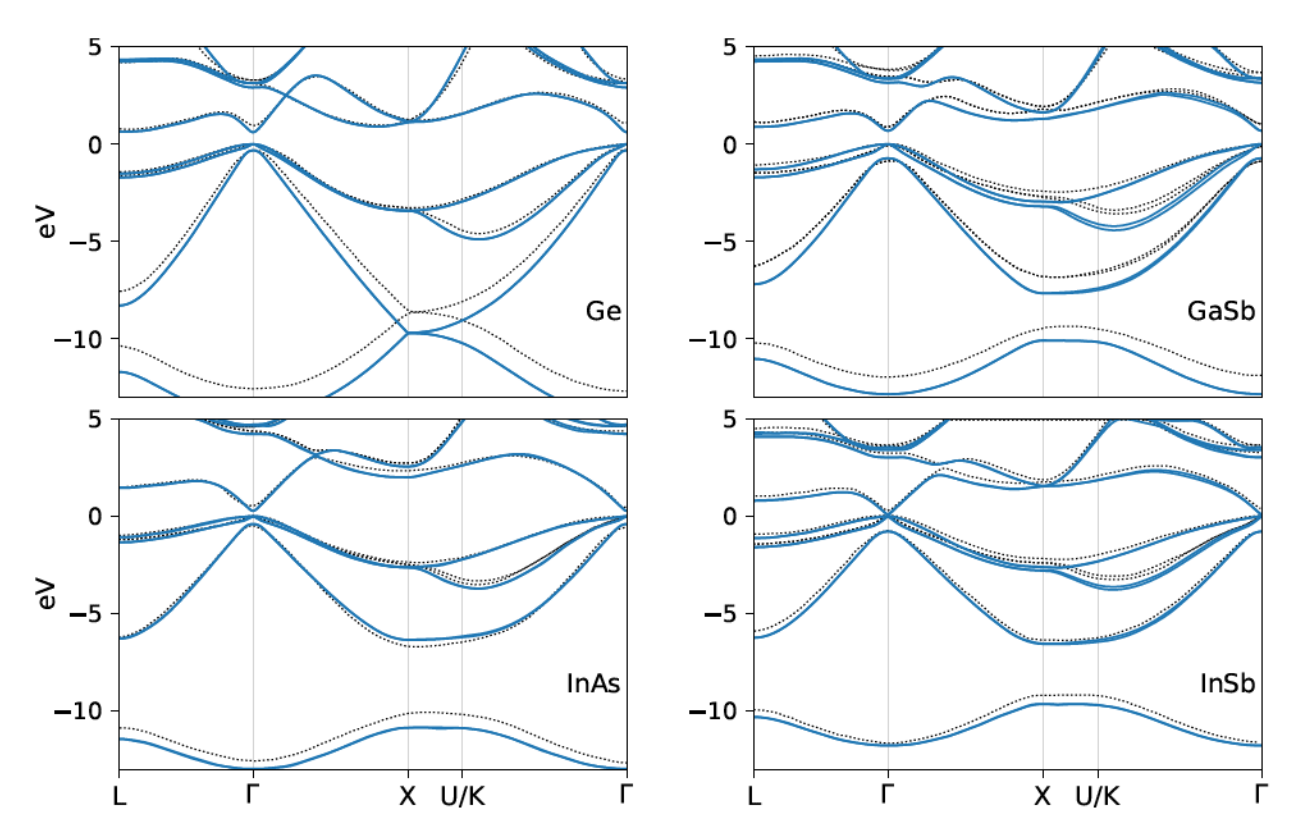


FIG. 1. Band structures, including spin-orbit coupling obtained from SRSH (with the range-separation parameter chosen to fit to the experimental band gap, blue solid lines) and the empirical pseudopotential method (black dotted lines) [69, 70].

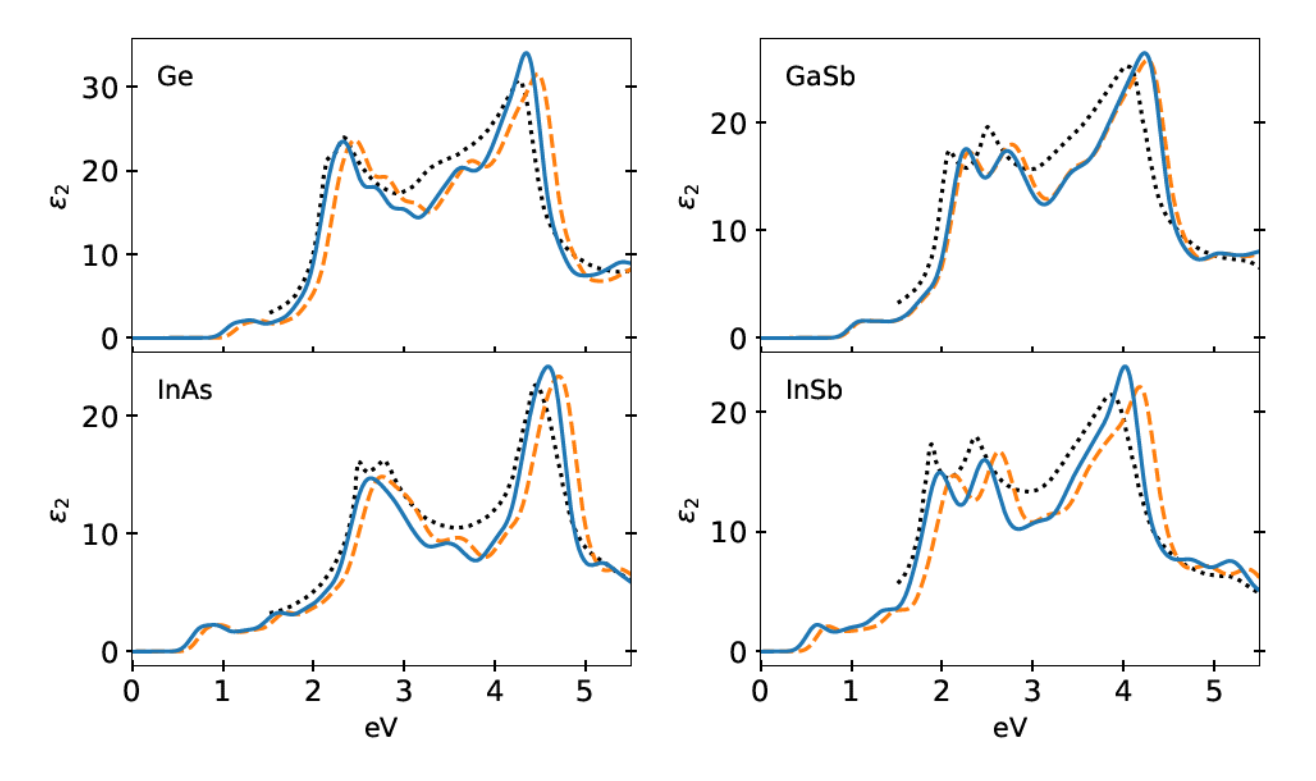


FIG. 2. Optical absorption spectra: SRSH with the range-separation parameter chosen to fit the experimental band gap (blue solid line), HSE (orange dashed line), and room temperature experimental data (black dotted line) [71]. Both SRSH and HSE data include spin-orbit coupling effects.

- [22] D. Waroquiers, A. Lherbier, A. Miglio, M. Stankovski, S. Poncé, M. J. T. Oliveira, M. Giantomassi, G.-M. Rignanese, and X. Gonze, Phys. Rev. B 87, 075121 (2013).
- [23] W. Chen and A. Pasquarello, Phys. Rev. B 90, 165133 (2014).
- [24] L. Leppert, T. Rangel, and J. B. Neaton, Phys. Rev. Materials 3, 103803 (2019).
- [25] J. Heyd, G. E. Scuseria, and M. Ernzerhof, J. Chem. Phys. 118, 8207 (2003); J. Heyd, *ibid.* 124, 219906 (2006).
- [26] Y. Hinuma, A. Grüneis, G. Kresse, and F. Oba, Phys. Rev. B 90, 155405 (2014).
- [27] Y.-S. Kim, K. Hummer, and G. Kresse, Phys. Rev. B 80, 035203 (2009).
- [28] S. Refaely-Abramson, S. Sharifzadeh, M. Jain, R. Baer, J. B. Neaton, and L. Kronik, Phys. Rev. B 88, 081204 (2013).
- [29] J. H. Skone, M. Govoni, and G. Galli, Phys. Rev. B 93, 235106 (2016).
- [30] W. Chen, G. Miceli, G.-M. Rignanese, and A. Pasquarello, Phys. Rev. Mater. 2, 073803 (2018).
- [31] G. Miceli, W. Chen, I. Reshetnyak, and A. Pasquarello, Phys. Rev. B 97, 121112 (2018).
- [32] T. Bischoff, I. Reshetnyak, and A. Pasquarello, Phys. Rev. B 99, 201114 (2019).
- [33] L. Kronik and S. Kümmel, Adv. Mater. 30, 1706560 (2018).
- [34] E. Runge and E. K. U. Gross, Phys. Rev. Lett. 52, 997 (1984).
- [35] N. T. Maitra, J. Chem. Phys. 144, 220901 (2016).
- [36] C. A. Ullrich, Time-dependent density-functional theory: concepts and applications (Oxford University Press, Oxford, 2011).
- [37] K. Burke, J. Chem. Phys. 136, 150901 (2012).
- [38] P. Ghosez, X. Gonze, and R. W. Godby, Phys. Rev. B 56, 12811 (1997).
- [39] Y.-H. Kim and A. Görling, Phys. Rev. Lett. 89, 096402 (2002).
- [40] F. Kootstra, P. L. de Boeij, and J. G. Snijders, Phys. Rev. B 62, 7071 (2000) Here the absorption spectra is shifted to match the real part of the dielectric response with experiment and this overcompensates for the redshift in the calculated spectra.
- [41] S. Botti, F. Sottile, N. Vast, V. Olevano, L. Reining, H.-C. Weissker, A. Rubio, G. Onida, R. Del Sole, and R. W. Godby, Phys. Rev. B 69, 155112 (2004).
- [42] S. Sharma, J. K. Dewhurst, A. Sanna, and E. K. U. Gross, Phys. Rev. Lett. 107, 186401 (2011).
- [43] V. U. Nazarov and G. Vignale, Phys. Rev. Lett. 107, 216402 (2011).
- [44] P. E. Trevisanutto, A. Terentjevs, L. A. Constantin, V. Olevano, and F. D. Sala, Phys. Rev. B 87, 205143 (2013).
- [45] Z. Ning, C.-T. Liang, and Y.-C. Chang, Phys. Rev. B 96, 085202 (2017).
- [46] A. V. Terentjev, L. A. Constantin, and J. M. Pitarke, Phys. Rev. B 98, 085123 (2018).
- [47] J. Paier, M. Marsman, and G. Kresse, Phys. Rev. B 78, 121201 (2008).
- [48] S. Refaely-Abramson, M. Jain, S. Sharifzadeh, J. B. Neaton, and L. Kronik, Phys. Rev. B 92, 081204 (2015).
- [49] Z.-h. Yang, F. Sottile, and C. A. Ullrich, Phys. Rev. B 92, 035202 (2015).
- [50] D. Wing, J. B. Haber, R. Noff, B. Barker, D. A. Egger,

- A. Ramasubramaniam, S. G. Louie, J. B. Neaton, and L. Kronik, Phys. Rev. Mater. 3, 064603 (2019).
- [51] J. Sun, J. Yang, and C. A. Ullrich, Phys. Rev. Research 2, 013091 (2020).
- [52] D. K. Lewis, A. Ramasubramaniam, and S. Sharifzadeh, Phys. Rev. Materials 4, 063803 (2020).
- [53] A. Tal, P. Liu, G. Kresse, and A. Pasquarello, Phys. Rev. Res. 2 (2020).
- [54] J. Sun and C. A. Ullrich, (2020), arXiv:2007.13711 [cond-mat.mtrl-sci].
- [55] A. M. Ferrari, R. Orlando, and M. Rérat, J. Chem. Theory Comput. 11, 3245 (2015).
- [56] J. P. Perdew, K. Burke, and M. Ernzerhof, Phys. Rev. Lett. 77, 3865 (1996).
- [57] G. Kresse and J. Furthmüller, Phys. Rev. B 54, 11169 (1996).
- [58] G. Kresse and D. Joubert, Phys. Rev. B 59, 1758 (1999).
- [59] R. W. Nunes and X. Gonze, Phys. Rev. B 63, 155107 (2001).
- [60] I. Souza, J. Íñiguez, and D. Vanderbilt, Phys. Rev. Lett. 89, 117602 (2002).
- [61] J. E. Northrup, M. S. Hybertsen, and S. G. Louie, Phys. Rev. Lett. 59, 819 (1987).
- [62] O. Madelung, Semiconductors Data Handbook, 3rd ed. (Springer-Verlag Berlin Heidelberg, 2004).
- [63] M. E. Casida, in Recent Advances in Density Functional Methods part I, edited by D. P. Chong (World Scientific, Singapore, 1995) Chap. 5, pp. 155–192.
- [64] M. Petersilka, U. J. Gossmann, and E. K. U. Gross, Phys. Rev. Lett. 76, 1212 (1996).
- [65] S. Tretiak and V. Chernyak, J. Chem. Phys. 119, 8809 (2003).
- [66] S. Hirata and M. Head-Gordon, Chem. Phys. Lett. 314, 291 (1999).
- [67] L. Kronik and J. B. Neaton, Annu. Rev. Phys. Chem. 67, 587 (2016), See section 2.
- [68] A. A. Mostofi, J. R. Yates, G. Pizzi, Y.-S. Lee, I. Souza, D. Vanderbilt, and N. Marzari, Comput. Phys. Commun. 185, 2309 (2014).
- [69] J. R. Chelikowsky and M. L. Cohen, Phys. Rev. B 14, 556 (1976).
- [70] M. L. Cohen and J. R. Chelikowsky, Electronic structure and optical properties of semiconductors, Vol. 75 (Springer Science & Business Media, 2012).
- [71] D. E. Aspnes and A. A. Studna, Phys. Rev. B 27, 985 (1983).
- [72] A. Joullié, A. Z. Eddin, and B. Girault, Phys. Rev. B 23, 928 (1981).
- [73] I. Vurgaftman, J. R. Meyer, and L. R. Ram-Mohan, J. appl. phys. 89, 5815 (2001).
- [74] S. M. Sze and K. K. Ng, Physics of semiconductor devices (John wiley & sons, 2006).
- [75] C. Kittel, P. McEuen, and P. McEuen, Introduction to solid state physics, Vol. 8 (Wiley New York, 1996) p. 185.
- [76] W. Hanke and L. J. Sham, Phys. Rev. Lett. 43, 387 (1979).